

# Multilayered Polyelectrolyte Films Containing Palladium Nanoparticles: Synthesis, Characterization, and Application in Selective Hydrogenation

Srividhya Kidambi and Merlin L. Bruening\*

Department of Chemistry, Michigan State University, East Lansing, Michigan 48824

Received September 13, 2004. Revised Manuscript Received October 27, 2004

Catalytic Pd nanoparticles in multilayer polyelectrolyte films can be easily prepared by alternating immersions of a substrate in  $\text{PdCl}_4^{2-}$  and polyethylenimine (PEI) solutions followed by chemical reduction of Pd(II) with  $\text{NaBH}_4$ . Transmission electron microscopy confirms that reduced  $[\text{PdCl}_4^{2-}/\text{PEI}]_3$  films contain nanoparticles with diameters of 1–4 nm, and X-ray photoelectron spectroscopy indicates that ~70% of the Pd in these films is Pd(0). Atomic emission analysis shows that little Pd is removed from  $\text{PdCl}_4^{2-}/\text{PEI}$  films during deposition of PEI or rinsing, but about 60% of the Pd in the film is leached during reduction by  $\text{NaBH}_4$ . In a system in which Pd(II) is deposited as a PEI complex, poly(acrylic acid) (PAA)/PEI–Pd(II) films, minimal leaching occurs during either reduction or deposition of PAA. Encapsulated nanoparticles in both  $[\text{PAA}/\text{PEI}–\text{Pd}(0)]_n\text{PAA}$  and reduced  $[\text{PdCl}_4^{2-}/\text{PEI}]_n$  films exhibit selective catalysis, as shown by the fact that Pd-catalyzed hydrogenation of allyl alcohol can occur an order of magnitude faster than hydrogenation of 3-methyl-1-penten-3-ol. Interestingly, adsorption of only  $\text{PdCl}_4^{2-}$  on alumina followed by reduction yields Pd that is 5-fold more active than commercial 5 wt % Pd on alumina. Without PEI, however, the catalyst is not selective. In  $[\text{PAA}/\text{PEI}–\text{Pd}(0)]_n\text{PAA}$  films, turnover frequency decreases with the number of layers deposited, suggesting that the outer layer of the film is primarily responsible for catalysis. In contrast, turnover frequency increases with the number of deposited layers for reduced  $[\text{PdCl}_4^{2-}/\text{PEI}]_n$  films. Selective diffusion through  $[\text{PdCl}_4^{2-}/\text{PEI}]_n$  membranes and first-order kinetics with respect to substrate concentration suggest that hydrogenation selectivities are due to different rates of transport to catalytic sites on the nanoparticles.

## Introduction

Metal nanoparticles are an interesting class of materials because they often exhibit properties different from those of the corresponding bulk metals.<sup>1–5</sup> For example, bulk Au is not catalytically active, but recent studies show that Au nanoparticles can serve as catalysts for oxidation and hydrogenation reactions.<sup>6–9</sup> Additionally, nanoparticle properties can be tuned by varying their sizes<sup>8,10,11</sup> and environments.<sup>12</sup> Because of these unique characteristics, metal nanoparticles are being intensively studied for applications

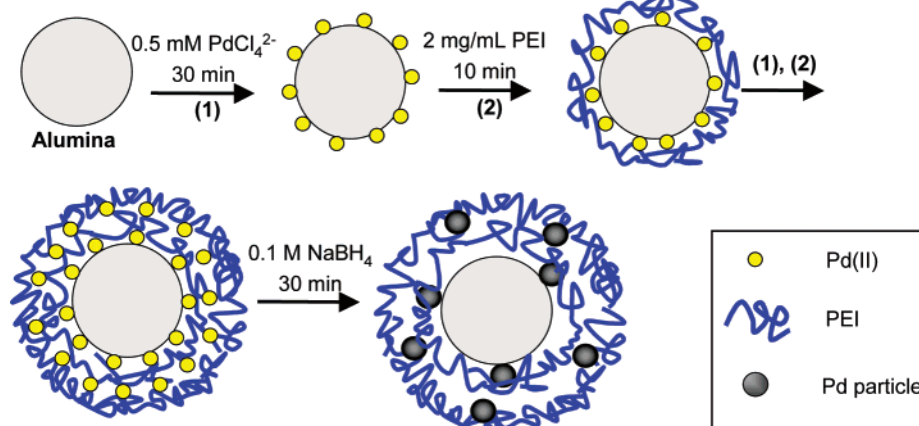
in catalysis,<sup>11,13</sup> optoelectronics,<sup>14</sup> preservatives,<sup>15</sup> and bio-sensing.<sup>16</sup>

Catalysis provides a natural application for nanoparticles because their large surface area-to-volume ratio allows effective utilization of expensive metals.<sup>17</sup> Without a suitable support, however, metal particles aggregate, reducing surface area and restricting control over particle size. To overcome this problem, catalytic nanoparticles have been immobilized on solid supports, e.g., carbon,<sup>18</sup> metal oxides,<sup>19</sup> and zeolites,<sup>20,21</sup> or stabilized by capping ligands that range from small organic molecules to large polymers.<sup>22–30</sup> Encapsulation by polymers is advantageous because in addition to

\* To whom correspondence should be addressed. E-mail: bruening@cem.msu.edu. Phone: 517-355-9715 x237. Fax: 517-353-1793.

- (1) Schmid, G. In *Nanoscale Materials in Chemistry*; Klabunde, K. J., Ed.; Wiley-Interscience: New York, 2001; pp 15–59.
- (2) Alvarez, M. M.; Khoury, J. T.; Schaaff, T. G.; Shafigullin, M. N.; Vezmar, I.; Whetten, R. L. *J. Phys. Chem. B* **1997**, *101*, 3706–3712.
- (3) Chen, S.; Ingram, R. S.; Hostetler, M. J.; Pietron, J. J.; Murray, R. W.; Schaaff, T. G.; Khoury, J. T.; Alvarez, M. M.; Whetten, R. L. *Science* **1998**, *280*, 2098–2101.
- (4) Quinn, B. M.; Liljeroth, P.; Ruiz, V.; Laaksonen, T.; Kontturi, K. *J. Am. Chem. Soc.* **2003**, *125*, 6644–6645.
- (5) Suzdalev, I. P.; Suzdalev, P. I. *Russ. Chem. Rev.* **2001**, *70*, 177–210.
- (6) Haruta, M. *Chem. Rev.* **2003**, *3*, 75–87.
- (7) Zanella, R.; Louis, C.; Giorgio, S.; Touroude, R. *J. Catal.* **2004**, *223*, 328–339.
- (8) Valden, M.; Lai, X.; Goodman, D. W. *Science* **1998**, *281*, 1647–1650.
- (9) Schimpf, S.; Lucas, M.; Mohr, C.; Rodemerck, U.; Bruckner, A.; Radnik, J.; Hofmeister, H.; Claus, P. *Catal. Today* **2002**, *72*, 63–78.
- (10) Rao, C. N. R.; Kulkarni, G. U.; Thomas, P. J.; Edwards, P. P. *Chem. – Eur. J.* **2002**, *8*, 28–35.
- (11) Li, Y.; Boone, E.; El-Sayed, M. A. *Langmuir* **2002**, *18*, 4921–4925.
- (12) Li, Y.; El-Sayed, M. A. *J. Phys. Chem. B* **2001**, *105*, 8938–8943.

- (13) Niu, Y.; Yeung, L. K.; Crooks, R. M. *J. Am. Chem. Soc.* **2001**, *123*, 6840–6846.
- (14) Park, J. H.; Lim, Y. T.; Park, O. O.; Kim, J. K.; Yu, J.-W.; Kim, Y. C. *Chem. Mater.* **2004**, *16*, 688–692.
- (15) Lee, J.-E.; Kim, J.-W.; Jun, J.-B.; Ryu, J.-H.; Kang, H.-H.; Oh, S.-G.; Suh, K.-D. *Colloid Polym. Sci.* **2004**, *282*, 295–299.
- (16) Ye, J.-S.; Ottova, A.; Tien, H. T.; Sheu, F.-S. *Bioelectrochemistry* **2003**, *59*, 65–72.
- (17) Fendler, J. H. *Nanoparticles and Nanostructured Films: Preparation, Characterization and Applications*; Wiley-VCH: Weinheim, Germany, 1998.
- (18) Liu, Z.; Ling, X. Y.; Su, X.; Lee, J. Y. *J. Phys. Chem. B* **2004**, *108*, 8234–8240.
- (19) Mallick, K.; Scurrell, M. S. *Appl. Catal., A* **2003**, *253*, 527–536.
- (20) Sun, C.; Peltre, M.-J.; Briand, M.; Blanchard, J.; Fajersberg, K.; Krafft, J.-M.; Breyse, M.; Cattenot, M.; Lacroix, M. *Appl. Catal., A* **2003**, *245*, 245–256.
- (21) Gurin, V. S.; Petranovskii, V. P.; Bogdanchikova, N. E. *Mater. Sci. Eng., C* **2002**, *19*, 327–331.
- (22) Bergbreiter, D. E.; Li, C. *Org. Lett.* **2003**, *5*, 2445–2447.
- (23) Kralik, M.; Biffis, A. *J. Mol. Catal. A* **2001**, *177*, 113–138.

Scheme 1. Formation of Pd Nanoparticles in  $[\text{PdCl}_4^{2-}/\text{PEI}]_n$  Films

stabilizing and protecting the particles, polymers offer unique possibilities for modifying both the environment around catalytic sites and access to these sites.<sup>23,31–35</sup> Hence, the protective polymer not only influences particle sizes and morphologies but can also have a tremendous influence on catalytic activity and selectivity.

We are developing catalytic nanoparticles embedded in multilayered polyelectrolyte films because the layer-by-layer deposition of these coatings, which simply involves alternating adsorption of polycations and polyanions, offers a versatile platform for potentially controlling catalyst properties.<sup>36–38</sup> There are two main strategies for preparing nanoparticle-containing polyelectrolyte films. In the first, the nanoparticles serve as the polycation or polyanion during film deposition,<sup>39,40</sup> whereas in the second, metal ions are incorporated into polyelectrolyte films and subsequently reduced to form nanoparticles (Scheme 1).<sup>41,42</sup> Either way,

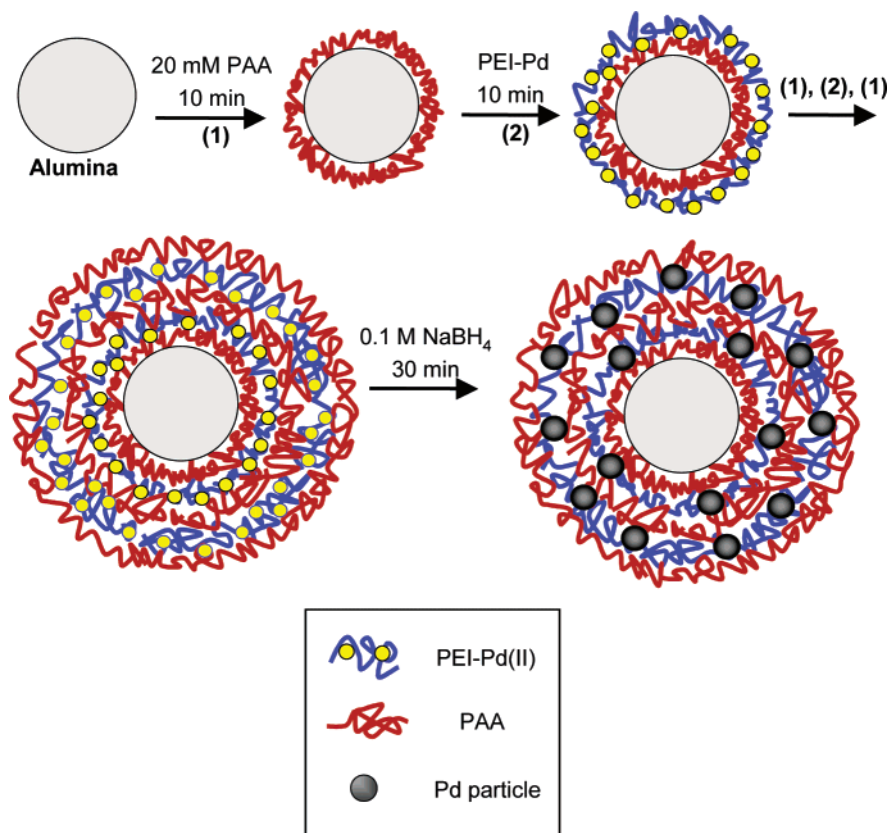
the simple layer-by-layer procedure permits deposition of films on nearly any surface, thus allowing the formation of catalytic systems on recoverable, high-surface-area substrates such as alumina. Moreover, because nearly any highly charged material can be used in alternating polyelectrolyte deposition, variation of constituent polyelectrolytes should allow tailoring of the nanoparticle environment as well as control over access to catalytic particles.

In a recent communication,<sup>43</sup> we described selective hydrogenation using Pd nanoparticles embedded in poly(acrylic acid) (PAA)/polyethylenimine (PEI) films. Here, we more fully examine the deposition, characterization, and catalytic properties of these films and also describe a new catalytic system that is prepared by alternating immersions of a substrate in  $\text{PdCl}_4^{2-}$  and PEI solutions followed by reduction of  $\text{Pd(II)}$  (Scheme 1).<sup>44,45</sup> This procedure builds on work by Watanabe and Regen that showed the deposition of dendrimer/ $\text{PtCl}_4^{2-}$  films,<sup>45</sup> as well as research by Liu et al. that demonstrated formation of Pd nanoparticles on glassy carbon by electrochemical reduction of films prepared by adsorption of  $\text{PdCl}_4^{2-}$  and an electroactive polycation.<sup>44</sup> Relative to Liu's procedure, we use a different polycation, and chemical, rather than electrochemical, reduction.

Nanoparticles in both  $[\text{PAA/PEI-Pd(0)}]_n\text{PAA}$  and reduced  $[\text{PdCl}_4^{2-}/\text{PEI}]_n$  films can catalyze hydrogenation of allyl alcohol at a rate that is an order of magnitude faster than hydrogenation of 3-methyl-1-penten-3-ol. However, the catalytic activities of the two systems as a function of the number of bilayers in the film are very different. The turnover frequency of  $[\text{PAA/PEI-Pd(0)}]_n\text{PAA}$  films decreases with an increasing number of bilayers, while the reduced  $[\text{PdCl}_4^{2-}/\text{PEI}]_n$  system shows the opposite trend. Hence, the reduced  $[\text{PdCl}_4^{2-}/\text{PEI}]_n$  system allows a significantly higher activity per g of catalyst (including the support) for multilayer films. This is likely due to greater accessibility of embedded particles in reduced  $\text{PdCl}_4^{2-}/\text{PEI}$  films.

- (24) Pathak, S.; Greci, M. T.; Kwong, R. C.; Mercado, K.; Prakash, G. K. S.; Olah, G. A.; Thompson, M. E. *Chem. Mater.* **2000**, *12*, 1985–1989.
- (25) Joly, S.; Kane, R.; Radzilowski, L.; Wang, T.; Wu, A.; Cohen, R. E.; Thomas, E. L.; Rubner, M. F. *Langmuir* **2000**, *16*, 1354–1359.
- (26) Underhill, R. S.; Liu, G. *Chem. Mater.* **2000**, *12*, 3633–3641.
- (27) Gopidas, K. R.; Whitesell, J. K.; Fox, M. A. *Nano Lett.* **2003**, *3*, 1757–1760.
- (28) Crooks, R. M.; Zhao, M.; Sun, L.; Chechik, V.; Yeung, L. K. *Acc. Chem. Res.* **2001**, *34*, 181–190.
- (29) Semagina, N. V.; Bykov, A. V.; Sulman, E. M.; Matveeva, V. G.; Sidorov, S. N.; Dubrovina, L. V.; Valetsky, P. M.; Kiselyova, O. I.; Khokhlov, A. R.; Stein, B.; Bronstein, L. M. *J. Mol. Catal. A* **2004**, *208*, 273–284.
- (30) Ye, H.; Scott, R. W. J.; Crooks, R. M. *Langmuir* **2004**, *20*, 2915–2920.
- (31) Mayer, A. B. R.; Mark, J. E. *J. Polym. Sci., Polym. Chem.* **1997**, *35*, 3151–3160.
- (32) Bonnemant, H.; Richards, R. M. *Eur. J. Inorg. Chem.* **2001**, 2455–2480.
- (33) Dante, S.; Advincula, R.; Frank, C. W.; Stroeve, P. *Langmuir* **1999**, *15*, 193–201.
- (34) Ciebiën, J. F.; Cohen, R. E.; Duran, A. *Supramol. Sci.* **1998**, *5*, 31–39.
- (35) Ciebiën, J. F.; Cohen, R. E.; Duran, A. *Mater. Sci. Eng., C* **1999**, *7*, 45–50.
- (36) Iler, R. K. *J. Colloid Interface Sci.* **1966**, *21*, 569–594.
- (37) Lvov, Y.; Decher, G.; Möhwald, H. *Langmuir* **1993**, *9*, 481–486.
- (38) Decher, G. *Science* **1997**, *277*, 1232–1237.
- (39) Schmitt, J.; Decher, G.; Dressick, W. J.; Brandow, S. L.; Geer, R. E.; Shashidhar, R.; Calvert, J. M. *Adv. Mater.* **1997**, *9*, 61–65.
- (40) Liu, Y.; Wang, Y.; Claus, R. O. *Chem. Phys. Lett.* **1998**, *298*, 315–319.
- (41) Wang, T. C.; Rubner, M. F.; Cohen, R. E. *Langmuir* **2002**, *18*, 3370–3375.

- (42) Dai, J.; Bruening, M. L. *Nano Lett.* **2002**, *2*, 497–501.
- (43) Kidambi, S.; Dai, J.; Li, J.; Bruening, M. L. *J. Am. Chem. Soc.* **2004**, *126*, 2658–2659.
- (44) Liu, J.; Cheng, L.; Song, Y.; Liu, B.; Dong, S. *Langmuir* **2001**, *17*, 6747–6750.
- (45) Watanabe, S.; Regen, S. L. *J. Am. Chem. Soc.* **1994**, *116*, 8855–8856.

Scheme 2. Formation of Pd Nanoparticles in  $[PAA/PEI-Pd(0)]_n PAA$  Films

### Experimental Section

**Materials.** Polyethylenimine (PEI) ( $M_w = 25\,000$ ), poly(acrylic acid) (PAA) (25 wt % in water,  $M_w = 90\,000$ ), poly(styrene sulfonate) (PSS) (sodium salt,  $M_w = 125\,000$ ), palladium (5 wt % on alumina powder),  $\alpha$ -alumina (100 mesh, typical particle size 75–100  $\mu\text{m}$ ), allyl alcohol (99%), 1-penten-3-ol (99%), 3-methyl-1-penten-3-ol (99%), and 3,4-dihydroxy-1-butene (99%) were purchased from Aldrich. Potassium tetrachloropalladate(II) (99.99%) was obtained from Alfa Aesar, and potassium chloride and sodium borohydride were acquired from Spectrum. All reagents were used as received, and solutions were prepared with deionized water (Milli-Q, 18.2  $M\Omega\text{ cm}$ ).

**Preparation of Pd Nanoparticles Encapsulated in Polyelectrolyte Films.** Synthesis of  $[PAA/PEI-Pd(0)]_n PAA$  films occurred as described previously.<sup>43</sup> Briefly, alternating immersion of alumina in solutions of PAA (20 mM, pH adjusted to 4.0) and a PEI–Pd(II) complex (1 mg/mL PEI, 2 mM  $K_2PdCl_4$ , pH adjusted to 9.0), followed by reduction of Pd(II) by  $NaBH_4$  yielded catalytic Pd nanoparticles in a PAA/PEI film (Scheme 2). Films were always capped with PAA and rinsed between the depositions of each polyelectrolyte. In a new method, we synthesized encapsulated Pd nanoparticles using alternating deposition of  $PdCl_4^{2-}$  and PEI on alumina particles and subsequent reduction of Pd(II) as depicted in Scheme 1.<sup>44</sup> Specifically, 15 g of  $\alpha$ -alumina was mixed with 100 mL of a solution containing 0.5 mM  $PdCl_4^{2-}$  and 0.1 M KCl, and the suspension was stirred vigorously for 30 min. Subsequently, the alumina was allowed to settle, and the supernatant was decanted. The alumina particles were then washed with three 100-mL aliquots of deionized water to remove excess  $PdCl_4^{2-}$ . To deposit a PEI layer, 100 mL of a PEI solution (2 mg/mL, pH adjusted to 9.0 with 1 M HCl) was added to the Pd(II)-coated alumina, and the particles were stirred for 10 min and washed as described above. Subsequent bilayers were deposited similarly. Reduction of Pd(II)

in these films was effected by exposure of the coated alumina to 100 mL of fresh 0.1 M  $NaBH_4$  for 30 min (with stirring). The reduced films were washed three times with water after exposure to  $NaBH_4$ . In some cases, alumina was first coated with PSS/PEI and then capped with  $PdCl_4^{2-}$ /PEI bilayers. The  $PdCl_4^{2-}$ /PEI was formed as described above, and the PSS/PEI precursor bilayers were deposited in a similar manner using a 10-min exposure to a PSS solution (20 mM PSS, 0.5 M  $MnCl_2$ , pH adjusted to 2.1) instead of  $PdCl_4^{2-}$ . All the catalysts were vacuum-dried after  $NaBH_4$  reduction, and no flocculation of the alumina was observed during deposition and rinsing. The coated alumina easily dispersed upon exposure to hydrogenation solutions.

**Characterization of Pd Nanoparticles.** Films  $[PEI/PdCl_4^{2-}]_n$  were also deposited on carbon-coated copper grids for transmission electron microscopy (TEM). Prior to film deposition, the grids were cleaned in a UV/ozone cleaner for 1 min, and TEM was performed on a JEOL 100CX microscope using an accelerating voltage of 100 kV. The digital images were taken with a Mega View III Soft Imaging System. Films were prepared using alternating 15-min immersions in 0.5 mM  $PdCl_4^{2-}$ , 0.1 M KCl, and 5-min immersions in 2 mg/mL PEI with 1-min water rinses between the two depositions. Nanoparticles formed upon reduction with 0.1 M  $NaBH_4$  for 15 min. We used somewhat shorter deposition times than those employed for the catalyst synthesis because of the small surface area of the TEM grid.

UV–Visible absorption spectra of  $[PEI/PdCl_4^{2-}]_n$  films on quartz slides were obtained using a Perkin-Elmer UV/Vis (model Lambda 40) spectrophotometer. To form films on quartz, slides were alternatively immersed into PEI and  $PdCl_4^{2-}$  solutions for 10 and 30 min, respectively, with a 1-min water rinse after each deposition. These depositions began with PEI rather than  $PdCl_4^{2-}$  because quartz is negatively charged at the pH values used in deposition. X-ray photoelectron spectroscopy (XPS) measurements were performed on coated alumina using a Physical Electronics PHI-



5400 ESCA workstation. Ellipsometric thicknesses of films on gold-coated wafers (200 nm of Au sputtered on 20 nm of Cr on Si(100)) were determined using a rotating analyzer ellipsometer (model M-44, J. A. Woollam), assuming a film refractive index of 1.5.

**Transport Studies.** Diffusion dialysis studies were performed using a home-built dialysis apparatus in which a porous alumina membrane (Whatman Anodisc, 0.02  $\mu\text{m}$  surface pores) coated with either  $[\text{PdCl}_4^{2-}/\text{PEI}]_{10}$  or  $[\text{PAA}/\text{PEI}]_7$  films was sandwiched between two glass cells.<sup>46</sup> More layers were used in these studies than in catalysis in order to cover the pores in the underlying alumina support. The source cell was filled with 90 mL of a 20 mM solution of the desired unsaturated alcohol (allyl alcohol, 1-penten-3-ol, 3-methyl-1-penten-3-ol, or 3,4-dihydroxy-1-butene), while the receiving cell initially contained 90 mL of deionized water. Both the source and the receiving sides were stirred vigorously to minimize concentration polarization at the membrane interface, and samples of the receiving phase were taken every 15 min and analyzed by gas chromatography (Shimadzu GC-17A equipped with an RTX-BAC1 column).

**Hydrogenation Reactions.** Catalytic hydrogenations were run in a 200-mL, three-neck, round-bottomed flask.  $\text{H}_2$  at a gauge pressure of 50 kPa was bubbled through a frit at the bottom of a solution that was vigorously stirred throughout the reaction. Suspensions of catalyst (250 mg) in  $\text{H}_2\text{O}$  (100 mL) were bubbled with  $\text{H}_2$  for 30 min before adding 2.0 mmol of substrate in 100 mL of water. Gas chromatography was used to analyze aliquots of the reaction mixture periodically. The sensitivity of the flame-ionization detector was assumed to be the same for products and reactants because they contain the same number of carbon atoms. (A spot check with allyl alcohol and 1-propanol showed this to be a good assumption.) GC-MS was used to identify compounds in reactions with multiple products.

**Determination of the Amount of Pd in Catalysts and Deposition Solutions.** Calculation of turnover frequencies (TOFs), i.e., the moles of substrate that are hydrogenated per mole of Pd per hour, requires knowledge of the amount of Pd in the catalyst. To determine Pd content, we employed atomic emission spectroscopy (Varian Spectra AA-200). Standard solutions (0.1 to 0.5 mM) were prepared by dissolving  $\text{K}_2\text{PdCl}_4$  in 0.1 M  $\text{HNO}_3$ , and sample solutions were prepared by stirring 250 mg of dried, synthesized catalyst in 2 mL of *aqua regia* for 15 min. These sample solutions were diluted to 12 mL with 0.1 M  $\text{HNO}_3$  and centrifuged (the  $\alpha$ -alumina support does not dissolve in *aqua regia*), and the supernatant was analyzed using its emission at 363.5 nm. When analyzing deposition solutions containing  $\text{K}_2\text{PdCl}_4$  in 0.1 M KCl, samples were diluted by a factor of 10, and standards were prepared in 0.01 M KCl rather than 0.1 M  $\text{HNO}_3$  to account for interferences from KCl.

## Results and Discussion

**Film Deposition.** In investigation of catalysis by nanoparticle-containing films, it is important to first understand film growth and composition. We performed UV/Vis spectroscopy of  $[\text{PEI}-\text{Pd}(\text{II})/\text{PAA}]_n$  and  $[\text{PEI}/\text{PdCl}_4^{2-}]_n$  films on quartz to demonstrate that layer-by-layer deposition occurs. As shown in Figure 1, the absorbance of  $\text{PEI}/\text{PdCl}_4^{2-}$  films at 220 nm, which is likely due to a  $\text{Pd}(\text{II})$ -amine charge-transfer band,<sup>13,47</sup> increases linearly with the number of bilayers. XPS spectra of  $\text{PEI}/\text{PdCl}_4^{2-}$  films show Cl-to-Pd ratios less than 1, so we think that Pd in these films is actually

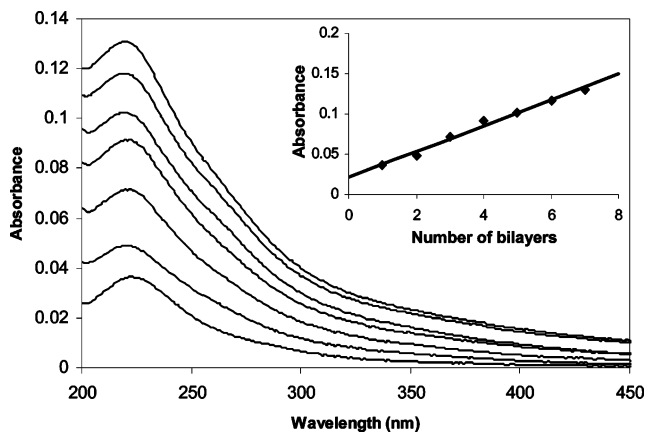


**Figure 1.** UV-Visible absorption spectra of  $[\text{PEI}/\text{PdCl}_4^{2-}]_n$  films on a quartz substrate with  $n = 1-7$  (from lower to upper curves). The inset shows the absorbance at  $\lambda_{\text{max}}$  (220 nm) vs the number of bilayers.

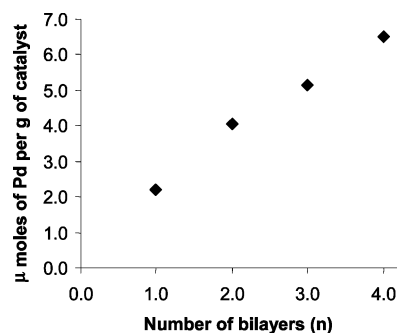


**Figure 2.** Micromoles of Pd (determined by atomic emission spectroscopy) per g of catalyst for several values of  $n$  in reduced  $[\text{PdCl}_4^{2-}/\text{PEI}]_n$  films deposited on alumina.

bound to PEI, and films are held together by metal-ion coordination.<sup>45,48</sup> (Thus the nomenclature  $\text{PEI}/\text{PdCl}_4^{2-}$  reflects deposition conditions and not the state of Pd in the films.) A linear increase in an absorbance peak at 222 nm also occurs with  $[\text{PEI}-\text{Pd}(\text{II})/\text{PAA}]_n$  (see Figure 1, Supporting Information), so UV/VIS spectra confirm the layer-by-layer growth of both  $[\text{PEI}/\text{PdCl}_4^{2-}]_n$  and  $[\text{PEI}-\text{Pd}(\text{II})/\text{PAA}]_n$  films.

To verify film growth on alumina particles, we performed atomic emission analysis of Pd. Figure 2 shows that the amount of Pd in  $[\text{PdCl}_4^{2-}/\text{PEI}]_n$  films increases linearly with the number of bilayers after deposition of the first layer, and similar results occur with  $[\text{PAA}/\text{PEI}-\text{Pd}(\text{II})]_n\text{PAA}$  (Figure 2, Supporting Information). We also analyzed the solutions employed in the deposition process to determine whether Pd was removed from films during rinsing, reduction, or deposition of PAA ( $[\text{PAA}/\text{PEI}-\text{Pd}(\text{II})]_n\text{PAA}$  films) or PEI ( $[\text{PdCl}_4^{2-}/\text{PEI}]_n$  films). On average, less than 10% of the amount of Pd deposited in the most recent step was leached from the catalyst during each deposition of PAA or PEI. Rinsing also leached very little Pd, but reduction with  $\text{NaBH}_4$  removed about 15% of the total Pd in  $[\text{PAA}/\text{PEI}-\text{Pd}]_n\text{PAA}$  coatings and 60% of the Pd in  $[\text{PdCl}_4^{2-}/\text{PEI}]_n$  films. Electrostatic interactions between PAA and PEI likely ionically cross-link  $[\text{PAA}/\text{PEI}-\text{Pd}]_n\text{PAA}$  films and help prevent removal of Pd. Another important point from atomic

(46) Stair, J. L.; Harris, J. J.; Bruening, M. L. *Chem. Mater.* **2001**, *13*, 2641-2648.

(47) Scott, R. W. J.; Ye, H.; Henriquez, R. R.; Crooks, R. M. *Chem. Mater.* **2003**, *15*, 3873-3878.

(48) Krass, H.; Papastavrou, G.; Kurth, D. G. *Chem. Mater.* **2003**, *15*, 196-203.

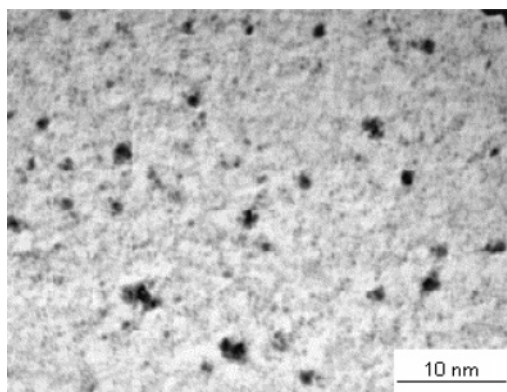


**Figure 3.** TEM image of a  $[\text{PdCl}_4^{2-}/\text{PEI}]_3$  film deposited on a carbon-coated copper grid and reduced with  $\text{NaBH}_4$ .

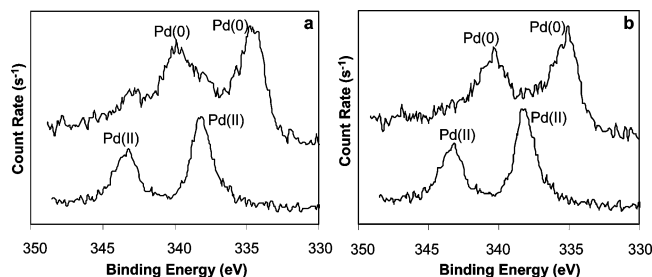


**Figure 4.** (a) XPS spectra of a  $[\text{PAA}/\text{PEI}-\text{Pd}]_3\text{PAA}$  film on alumina before (bottom) and after (top) reduction with  $\text{NaBH}_4$ . (b) Corresponding spectra of a  $[\text{PdCl}_4^{2-}/\text{PEI}]_3$  film on alumina.

emission results is that because of the high surface area of the alumina, deposition solutions do lose around 60% of their Pd to adsorption. Thus, we used fresh solutions for each deposition step.

**Film Characterization.** To investigate the reduction of  $\text{Pd(II)}$  to form nanoparticles, we performed both TEM and XPS. The TEM image in Figure 3 confirms the formation of Pd nanoparticles during exposure of  $[\text{PdCl}_4^{2-}/\text{PEI}]_3$  films to  $\text{NaBH}_4$ . The particles have diameters of 1–4 nm and are distributed throughout the film. (We note that there may be particles with diameters  $<1$  nm, but these would be difficult to see and likely unstable.) The Supporting Information contains a histogram of particle sizes  $>1$  nm. Our prior studies of  $\text{PAA}/\text{PEI}-\text{Pd(0)}$  films showed a similar distribution of nanoparticles with sizes ranging from 1 to 3 nm.<sup>43</sup> The ellipsometric thicknesses of  $[\text{PEI}/\text{PAA}]_3\text{PEI}$  and  $[\text{PEI}/\text{PdCl}_4^{2-}]_3$  films on gold-coated Si wafers were 125 and 65 Å, respectively. Thicknesses on the carbon-coated Cu grid should be similar, so TEM images should probe the entire depth of the film.

XPS provides information about the Pd oxidation state in reduced  $\text{PdCl}_4^{2-}/\text{PEI}$  and  $\text{PAA}/\text{PEI}-\text{Pd(0)}$  films because photoelectrons with energies of 337 and 342 eV correspond to  $\text{Pd(II)}$ , while those at 335 and 340 eV correspond to  $\text{Pd(0)}$ .<sup>49</sup> Figure 4 contains the XPS spectra of  $[\text{PAA}/\text{PEI}-\text{Pd}]_3\text{PAA}$  and  $[\text{PdCl}_4^{2-}/\text{PEI}]_3$  films on alumina before and after reduction with  $\text{NaBH}_4$ . These spectra indicate that approximately 70% of the Pd in these films is reduced from  $\text{Pd(II)}$  to  $\text{Pd(0)}$  upon exposure to  $\text{NaBH}_4$ . The incomplete reduction could arise due to inaccessibility of a few Pd ions

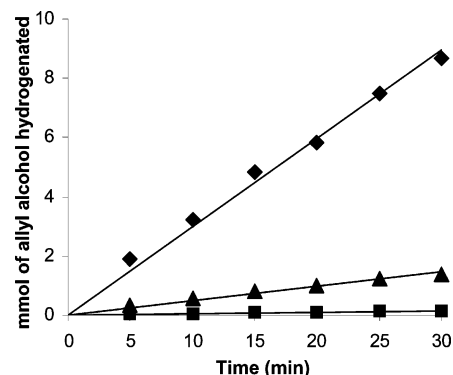


**Figure 5.** Amount of allyl alcohol hydrogenated vs reaction time for 200-mL solutions initially containing 20 mmol (diamonds), 2 mmol (triangles), and 0.2 mmol (squares) of allyl alcohol. The catalyst was 250 mg of alumina coated with a reduced  $[\text{PdCl}_4^{2-}/\text{PEI}]_3$  film.

to  $\text{NaBH}_4$  or air oxidation of a small amount of  $\text{Pd(0)}$ .<sup>47</sup> (Given the thicknesses of these films and a sampling depth in XPS of about 100 Å, most of the film is being probed in these measurements. However, XPS is not capable of probing films adsorbed in the alumina pores).

**Catalysis of Hydrogenation.** To investigate some of the catalytic properties of reduced Pd in polyelectrolyte films, we hydrogenated a series of unsaturated alcohols using the nanoparticles as catalysts. We studied hydrogenation rates as a function of substrate concentration and film composition to probe the reaction as well as film structure.

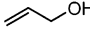
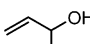
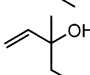
**Reaction Kinetics.** Figure 5 demonstrates how the rate of allyl alcohol hydrogenation catalyzed by reduced  $[\text{PdCl}_4^{2-}/\text{PEI}]_3$  on alumina varies with initial allyl alcohol concentration. Increasing the concentration of allyl alcohol by a factor of 10 gives on average a 9-fold increase in TOF, implying a reaction order of  $\sim 1$ . Similar kinetics (approximately first order) were observed with the  $\text{PAA}/\text{PEI}-\text{Pd(0)}$  system.<sup>43</sup> In reactions with conventional Pd catalysts, hydrogenation is typically zero order with respect to substrate concentration, probably because the Pd in such catalysts is saturated with substrate.<sup>29,50</sup> In contrast, for nanoparticles in polyelectrolyte multilayers, the first-order kinetics suggest that the rate-limiting step involves either diffusion of the substrate to the nanoparticles or slow adsorption. Selectivities among substrates and the transport studies discussed below indicate that diffusion may be the rate-limiting process in these reactions.

**Catalytic Activity of Reduced  $[\text{PdCl}_4^{2-}/\text{PEI}]_n$  as a Function of the Substrate and Film Composition.** Table 1 summarizes the TOFs for catalysis of hydrogenation of several substrates by reduced  $[\text{PdCl}_4^{2-}/\text{PEI}]_n$  films. The substrates for hydrogenation, allyl alcohol (**1**), 1-penten-3-ol (**2**), and 3-methyl-1-penten-3-ol (**3**), differ only in the substituents at the  $\alpha$ -carbon of the double bond, but with reduced  $[\text{PdCl}_4^{2-}/\text{PEI}]_4$  films as catalysts, hydrogenation rates for **1** are 11-fold higher than those for **3**. For alumina coated with only reduced  $\text{PdCl}_4^{2-}$  ( $n = 0.5$ ), TOFs are very high, but reaction rates for the different substrates vary by a factor of less than 1.4. This shows that the presence of additional alkyl groups at the  $\alpha$ -carbon does not significantly alter reactivity. Thus, the selectivity of hydrogenation using reduced  $\text{PdCl}_4^{2-}/\text{PEI}$

(49) Kumar, G.; Blackburn, J. R.; Albridge, R. G.; Moddeman, W. E.; Jones, M. M. *Inorg. Chem.* **1972**, *11*, 296–300.

(50) Yoon, C.; Yang, M. X.; Somorjai, G. A. *Catal. Lett.* **1997**, *46*, 37–41.

**Table 1. Hydrogenation TOFs (Moles Hydrogenated per Mole of Pd per Hour) for Different Catalysts**

	5% Pd/Al <sub>2</sub> O <sub>3</sub> <sup>a</sup>	Reduced [PdCl <sub>4</sub> <sup>2-</sup> /PEI] <sub>n</sub> catalysts on alumina for several values of n <sup>b</sup>					
		n = 0.5 <sup>c</sup>	n = 1	n = 2	n = 3	n = 4	1.0 + 2.0 <sup>d</sup>
1 	1300±150	5880/6130	820/670	750/1100	1990/1670	1220/1630	720/750
2 	1500±120	5570/5940	230/190	240/440	690/530	450/540	250/280
3 	1500±100	4250/4720	190/140	110/150	260/170	110/150	50/70

<sup>a</sup> TOF values for commercially available 5%-Pd-on-alumina catalyst are from ref 43. <sup>b</sup> Values are given for replications of the same reaction with two different batches of catalyst. Small, random differences in the film formation processes may account for the variations in TOFs. The hydrogenation solution originally contained 2.0 mmol of unsaturated alcohol in 200 mL of water, and the TOF represents the initial rate. <sup>c</sup> This film was prepared by adsorption of only PdCl<sub>4</sub><sup>2-</sup> and subsequent reduction with NaBH<sub>4</sub>. <sup>d</sup> Reduced [PSS/PEI]<sub>1</sub>/[PdCl<sub>4</sub><sup>2-</sup>/PEI]<sub>2</sub>.

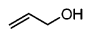
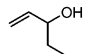
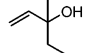
films does not stem from differences in the electronic properties of the substrates.

With a commercially available 5%-Pd-on-alumina catalyst (Aldrich), hydrogenation rates for the three unsaturated alcohols are also very close ( $1/2 \approx 1/3 = 0.87$ ).<sup>43</sup> However, TOFs are 4-fold lower for the commercial catalyst than for the reduced PdCl<sub>4</sub><sup>2-</sup> ( $n = 0.5$ ) system. The high activity of reduced PdCl<sub>4</sub><sup>2-</sup> on alumina may result from small Pd nanoparticles with a large surface area, but we should note that the Pd loading in these catalysts is only 0.034 wt %. Hence, rates of hydrogenation per g of catalyst (including the support) are still ~40-fold higher with the commercial 5%-Pd-on-alumina.

Relative to the reduced PdCl<sub>4</sub><sup>2-</sup> ( $n = 0.5$ ) catalyst, the presence of a PEI layer in a reduced [PdCl<sub>4</sub><sup>2-</sup>/PEI]<sub>1</sub> system decreases the TOF for allyl alcohol by a factor of ~8. The decrease in TOF is more appreciable for **2** and **3**, resulting in **1/2** and **1/3** average selectivities of 3.5 and 4.6, respectively. The decrease in rates after PEI adsorption could occur in part because Pd nanoparticles that are present in the alumina pores become inaccessible after coating with a layer of PEI. In addition, the PEI likely provides selectivity by controlling the rate of transport to accessible nanoparticles. The possible presence of inaccessible Pd in alumina pores might explain why the TOF for allyl alcohol increases on going from [PdCl<sub>4</sub><sup>2-</sup>/PEI]<sub>1</sub> to [PdCl<sub>4</sub><sup>2-</sup>/PEI]<sub>3</sub> or [PdCl<sub>4</sub><sup>2-</sup>/PEI]<sub>4</sub> catalysts. Inaccessible Pd would decrease the TOF for all of the films, but the fraction of Pd that is in the substrate pores should be less for thicker films. Because the initial bilayer contains nearly 2-fold more Pd than the 3rd and 4th bilayers (see Figure 2), the effect of inaccessible Pd could be significant. Eventually, however, decreases in TOFs due to longer transport pathways to underlying layers should overcome the fact that the fraction of Pd that is inaccessible in support pores decreases with an increasing number of bilayers.

In an effort to understand whether inactive Pd nanoparticles in the support decrease the activity of the catalyst, we examined catalysis by reduced [PSS/PEI]<sub>1</sub>/[PdCl<sub>4</sub><sup>2-</sup>/PEI]<sub>2</sub> coatings. We thought that these films would have a higher TOF than reduced [PdCl<sub>4</sub><sup>2-</sup>/PEI]<sub>2</sub> films, since the initial bilayer of PSS/PEI could cover the pores of alumina (at least partially) and decrease deposition of inaccessible Pd. However, TOFs of reduced [PSS/PEI]<sub>1</sub>/[PdCl<sub>4</sub><sup>2-</sup>/PEI]<sub>2</sub> films are

**Table 2. Hydrogenation TOFs for Catalysts Containing [PAA/PEI-Pd(0)]<sub>n</sub>PAA Films on Alumina with Several Values of *n***

		n = 1 <sup>a</sup>	n = 2 <sup>a</sup>	n = 3 <sup>b</sup>
1 		2130/2150	1260/1170	730±130
2 		810/970	370/380	280±20
3 		280/350	130/120	60±15

<sup>a</sup> Values are given for replications of the same reaction with two different batches of catalyst. The hydrogenation solution originally contained 2.0 mmol of unsaturated alcohol in 200 mL of water, and the TOF represents the initial rate. <sup>b</sup> TOF values from ref 43.

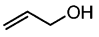
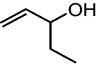
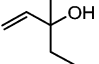
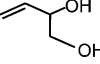
about the same or slightly lower than those of reduced [PdCl<sub>4</sub><sup>2-</sup>/PEI]<sub>2</sub> films (Table 1). With reduced [PSS/PEI]<sub>4</sub>/[PdCl<sub>4</sub><sup>2-</sup>/PEI]<sub>2</sub> films, TOF decreased even further (TOF of 330 for allyl alcohol). Decreases in TOF could occur because of penetration of Pd into the precursor layer,<sup>51</sup> which also might explain the increased deposition of Pd in [PSS/PEI]<sub>1</sub>/[PdCl<sub>4</sub><sup>2-</sup>/PEI]<sub>2</sub> and [PSS/PEI]<sub>4</sub>/[PdCl<sub>4</sub><sup>2-</sup>/PEI]<sub>2</sub> films ( $1.4 \times 10^{-6}$  moles in 250 mg of catalyst for both systems) relative to [PdCl<sub>4</sub><sup>2-</sup>/PEI]<sub>2</sub> films ( $1.0 \times 10^{-6}$  moles in 250 mg). Another explanation for the lower turnover frequency in reduced [PSS/PEI]<sub>1</sub>/[PdCl<sub>4</sub><sup>2-</sup>/PEI]<sub>2</sub> and [PSS/PEI]<sub>4</sub>/[PdCl<sub>4</sub><sup>2-</sup>/PEI]<sub>2</sub> films might be the intermingling of PSS in PdCl<sub>4</sub><sup>2-</sup>/PEI layers,<sup>38</sup> which would likely yield a more ionically cross-linked, less permeable film.

**Catalytic Activity of Reduced [PAA/PEI-Pd(0)]<sub>n</sub>PAA as a Function of the Substrate and Film Composition.** We thought that the catalytic activity of Pd in [PAA/PEI-Pd(0)]<sub>n</sub>PAA would be lower than that in reduced PdCl<sub>4</sub><sup>2-</sup>/PEI because the PAA should help to restrict access to Pd nanoparticles. Table 2 shows that TOFs of [PAA/PEI-Pd(0)]<sub>3</sub>PAA films are indeed about half of those for reduced [PdCl<sub>4</sub><sup>2-</sup>/PEI]<sub>3</sub> and [PdCl<sub>4</sub><sup>2-</sup>/PEI]<sub>4</sub> films. However, unlike the [PdCl<sub>4</sub><sup>2-</sup>/PEI]<sub>n</sub> system, the TOFs of [PAA/PEI-Pd(0)]<sub>n</sub>PAA films decrease with an increasing number of bilayers. This decrease in TOF reflects an approximately linear increase in Pd content with an increasing number of bilayers (see Figure 2, Supporting Information) along with a relatively constant reaction rate. The initial deposition of PAA and the binding of Pd to PEI should minimize

(51) Caruso, F.; Kurth, D. G.; Volkmer, D.; Koop, M. J.; Mueller, A. *Langmuir* **1998**, *14*, 3462–3465.



**Table 3. Hydrogenation TOFs for Reduced  $[\text{PdCl}_4^{2-}/\text{PEI}]_3$  Films on Alumina**

		TOF <sup>a</sup>
1		1990/1670
2		690/530
3		260/170
4		940/740

<sup>a</sup> Values are given for replications of the same reaction with two different batches of catalyst. The hydrogenation solution originally contained 2.0 mmol of unsaturated alcohol in 200 mL of water, and the TOF represents the initial rate.

deposition of Pd in alumina pores in this system. Thus, the regular decrease in turnover frequency with the addition of more bilayers most likely shows that with  $[\text{PAA}/\text{PEI}-\text{Pd}(0)]_n\text{PAA}$ , the hydrogenation reaction is effected primarily by Pd nanoparticles present in the outermost layer of the catalyst. Ionic cross-linking in  $[\text{PAA}/\text{PEI}-\text{Pd}(0)]_n\text{PAA}$  films likely restricts access to inner portions of the film. In contrast, reduced  $[\text{PdCl}_4^{2-}/\text{PEI}]_n$  coatings probably allow catalysis throughout the film, and thus this multilayered system gives a significantly higher activity per g of catalyst (including the support).

**Roles of Size and Polarity in Selectivity.** The molecules listed in Tables 1 and 2 differ in size, but they also differ in polarity. To investigate whether selectivities are due primarily to polarity or size effects, we examined hydrogenation of 3,4-dihydroxy-1-butene (**4**). Table 3 shows the TOFs for hydrogenation of **1–4** using alumina coated with reduced  $[\text{PdCl}_4^{2-}/\text{PEI}]_3$  films. Even though **4** is more polar than **2**, the TOFs of these two substrates are within 30% of each other, suggesting that size is the primary factor controlling the rate of hydrogenation.

**Transport Studies.** To better understand the mechanism behind selective hydrogenation by encapsulated nanoparticles, we examined substrate diffusion through a porous alumina membrane (0.02- $\mu\text{m}$  pore size) coated with unreduced  $[\text{PdCl}_4^{2-}/\text{PEI}]_{10}$  films. The ratios of transport rates for **1/2**, **1/4**, and **1/3** were about 1.7, 2.0, and 3.1, respectively. Transport studies performed with reduced  $[\text{PdCl}_4^{2-}/\text{PEI}]_7$  films on porous alumina showed selectivities similar to those of the nonreduced films. The transport experiments suggest

that differential rates of diffusion to the Pd nanoparticles could play a role in selective catalysis, but the diffusion dialysis selectivities are 3- to 4-fold lower than catalytic selectivities of reduced  $[\text{PdCl}_4^{2-}/\text{PEI}]_4$ . We surmise that both diffusion through  $[\text{PdCl}_4^{2-}/\text{PEI}]_n$  films and access to Pd nanoparticles rely on specific paths through the polyelectrolyte matrix. Selective diffusion of substrates to active sites on nanoparticles may not be completely reflected in diffusion dialysis, because transport through a  $[\text{PdCl}_4^{2-}/\text{PEI}]_n$  membrane could bypass embedded particles.

In the case of  $\text{PAA}/\text{PEI}-\text{Pd}$ , diffusion studies through an alumina membrane coated with a  $[\text{PAA}/\text{PEI}]_7$  film were already reported.<sup>43</sup> The ratios of the transport rates through such membranes are about 4 for **1/2** and 15 for **1/3**. In this system, catalytic selectivities are quite similar to transport selectivities, suggesting that diffusion does control reaction rates.

## Conclusions

Deposition of Pd(II) in polyelectrolyte films followed by reduction yields catalytic, nanoparticle-containing films, and such films can serve as selective catalysts in the hydrogenation of small, unsaturated alcohols. For  $[\text{PAA}/\text{PEI}-\text{Pd}(0)]_n\text{PAA}$  films, TOFs decrease with the number of bilayers, suggesting that mainly the outer layers of the film effect catalysis. However, TOFs for reduced  $[\text{PdCl}_4^{2-}/\text{PEI}]_n$  films show the opposite trend, demonstrating that there are structural differences between these two catalytic systems. Transport studies and reaction orders suggest that catalytic selectivities are due to selective diffusion of the reactant molecules to catalytic sites, and selective access is primarily a function of substrate size, not polarity.

**Acknowledgment.** We gratefully acknowledge the American Chemical Society Petroleum Research Fund for supporting this work. We also thank Dr. Per Askeland for his assistance in XPS studies and Professor David Bergbreiter (Texas A&M University) for helpful suggestions.

**Supporting Information Available:** UV–Visible absorption spectra of  $[\text{PEI}-\text{Pd}(\text{II})/\text{PAA}]_n$  films, atomic emission spectroscopy data for  $[\text{PAA}/\text{PEI}-\text{Pd}(0)]_n\text{PAA}$  catalysts, and a histogram of particle sizes obtained from a TEM image of a reduced  $[\text{PdCl}_4^{2-}/\text{PEI}]_3$  film (pdf). This information is available free of charge via the Internet at <http://pubs.acs.org>.

CM048421T